NMR Mapping and Secondary Structure Determination of the Major Acetylcholine Receptor α-Subunit Determinant Interacting with α-Bungarotoxin[†,‡]

Abraham O. Samson,[§] Jordan H. Chill,[§] Erik Rodriguez,[§] Tali Scherf,[||] and Jacob Anglister*[,§]

Department of Structural Biology and Chemical Services, The Weizmann Institute of Science, Rehovot 76100, Israel

Received September 26, 2000; Revised Manuscript Received January 23, 2001

ABSTRACT: The α-subunit of the nicotinic acetylcholine receptor (αAChR) contains a binding site for α-bungarotoxin (α-BTX), a snake-venom-derived α-neurotoxin. Previous studies have established that the segment comprising residues 173−204 of αAChR contains the major determinant interacting with the toxin, but the precise boundaries of this determinant have not been clearly defined to date. In this study, we applied NMR dynamic filtering to determine the exact sequence constituting the major αAChR determinant interacting with α-BTX. Two overlapping synthetic peptides corresponding to segments 179−200 and 182−202 of the αAChR were complexed with α-BTX. HOHAHA and ROESY spectra of these complexes acquired with long mixing times highlight the residues of the peptide that do not interact with the toxin and retain considerable mobility upon binding to α-BTX. These results, together with changes in the chemical shifts of the peptide protons upon complex formation, suggest that residues 184−200 form the contact region. At pH 4, the molecular mass of the complex determined by dynamic light scattering (DLS) was found to be 11.2 kDa, in excellent agreement with the expected molecular mass of a 1:1 complex, while at pH >5 the DLS measurement of 20 kDa molecular mass indicated dimerization of the complex. These results were supported by T_2 measurements. Complete resonance assignment of the 11.2 kDa complex of α-BTX bound to the αAChR peptide comprising residues 182−202 was obtained at pH 4 using homonuclear 2D NMR spectra measured at 800 MHz. The secondary structures of both α-BTX and the bound αAChR peptide were determined using 2D ^{1}H NMR experiments. The peptide folds into a β-hairpin conformation, in which residues ^{R}H186−^{R}V188 and ^{R}Y198−^{R}D200 form the two β-strands. Residues ^{R}Y189−^{R}T191 form an intermolecular β-sheet with residues ^{B}K38−^{B}V40 of the second finger of α-BTX. These results accurately pinpoint the α-BTX-binding site on the αAChR and pave the way to structure determination of this important αAChR determinant involved in binding acetylcholine and cholinergic agonists and antagonists.

The nicotinic acetylcholine receptor (AChR)[1] is a ligand-gated ion channel that is activated upon binding of acetylcholine. It is a 290 kDa membrane glycoprotein found in muscle and neuronal tissues consisting of five homologous subunits in the stoichiometry of $\alpha_2\beta\delta\gamma$ or $\alpha_2\beta\delta\epsilon$ (*1*−*3*). Located on the postsynaptic surface of the neuromuscular junction, the AChR translates the chemical signal of acetylcholine binding into an electrical one, leading to muscle contraction. The acetylcholine-binding site is formed by the $\alpha\delta$ and $\alpha\gamma$ subunits (*4*). The α-subunit also contains a high-affinity-binding site for α-neurotoxin antagonists (*5*, *6*), as well as the major immunogenic region (MIR), which is the main target of autoimmune antibodies in myasthenia gravis (*7*−*9*). α-Bungarotoxin (α-BTX) is a 74 amino acid, 8 kDa α-neurotoxin derived from the venom of *Bungarus multicinctus*. It binds to the postsynaptic muscle AChR with a K_D of 10^{-11} M (*10*), competitively inhibiting acetylcholine binding, thereby preventing the depolarizing action on postsynaptic membranes and blocking neuromuscular transmission (*11*). Electron microscopy (*12*−*14*) and photolabeling experiments indicate that the binding site for α-BTX is restricted mostly to the α-subunit (*15*, *16*), and partially overlaps that of acetylcholine (*17*−*19*). αAChR isolated from *Torpedo californica* binds α-BTX even after denaturation, indicating that a contiguous segment of this subunit forms a binding site for α-BTX (*15*). A major determinant of the toxin-binding site was mapped to residues 173−204 of αAChR (*20*). A 32 residue peptide corresponding to this segment binds α-BTX with a K_D of 1.4×10^{-7} M, which is

[†] This study was supported by a US−Israel Binational Science Foundation Grant 98-328 to J.A.

[‡] The chemical shifts have been deposited in BioMagResBank under accession number 4838.

* To whom correspondence should be addressed. J.A. is the Dr. Joseph and Ruth Owades Professor of Chemistry. Tel: 972 8 9343394, Fax: 972 8 9344136, E-mail: Jacob.Anglister@weizmann.ac.il.

[§] Department of Structural Biology.

[||] Chemical Services.

[1] Abbreviations: AChR, nicotinic acetylcholine receptor; αAChR, α-subunit of AChR; α-BTX, α-bungarotoxin; NMR, nuclear magnetic resonance; 2D-NMR, two-dimensional NMR; HOHAHA, homonuclear Hartmann−Hahn spectroscopy; NOE, nuclear Overhauser effect; NOESY, nuclear Overhauser spectroscopy; ROESY, rotating-frame Overhauser spectroscopy; DQF−COSY, double-quantum-filtered correlation spectroscopy; $T_{1\rho}$, spin−lattice relaxation time in the rotating frame; T_2, transverse relaxation time constant; CD, circular dichroism; DLS, dynamic light scattering; FPLC, fast protein liquid chromatography; RP-HPLC, reverse-phase high-pressure liquid chromatography; IC_{50}, concentration of competing inhibitor resulting in a 50% decrease in binding of the assayed ligand; α-BTX and αAChR peptide residues are designated by a superscript B (^{B}X) and R (^{R}X), respectively, before the one-letter amino acid code and position in the sequence.

10.1021/bi0022689 CCC: $20.00
Published on Web 04/11/2001

comparable to the affinity of the intact denatured αAChR to the toxin (*21*, *22*). Several studies have focused upon the α-BTX affinity to αAChR synthetic peptide analogues in an attempt to locate the α-BTX-binding domain on the receptor more precisely. These studies suggest various putative binding domains within the aforementioned 32 amino acid peptide such as residues 185−199 (*23*), 181−200 (*24*), 179−196 (*21*, *22*), 184−200 (*25*), and 185−196 (*26*). Concurrently, site-directed mutagenesis and affinity labeling studies have pinpointed residues within this domain critical to acetylcholine and antagonist binding (*27*, *28*).

Complexes of αAChR peptide analogues with α-BTX have also been the subject of structural studies. The solution structure of α-BTX in complex with a dodecapeptide, KHWVYYTCCPDT, corresponding to residues 185−196 of *Torpedo* αAChR, was solved by Basus and co-workers using NMR (*29*). They established interactions between α-BTX and the segment corresponding to residues 186−190 of the αAChR, yet no interactions were detected for the C-terminal half of the peptide. Thus, the short peptide studied by Basus and co-workers represents only a fraction of the α-BTX-binding domain in αAChR.

Anglister, Katchalski-Katzir, and co-workers (*30*) recently determined the three-dimensional solution structure of α-BTX in complex with a 13 residue peptide (MRYYESSLKSYPD) selected from a phage-displayed peptide library. This complex is of special interest, since this tridecapeptide exhibits a 15-fold higher affinity to α-BTX in comparison to the dodecapeptide αAChR used by Basus et al. While the peptide corresponding to residues 185−196 of αAChR adopts an extended conformation when bound to the toxin (*29*), the toxin-bound library peptide is nearly globular and occupies a larger surface area of the α-BTX-binding site. In view of the larger number of interactions and the 15-fold higher binding constant for the library peptide, the globular conformation of this peptide seems to mimic a larger αAChR determinant, and provides a more detailed picture of the α-BTX-binding site for AChR.

Despite these recent advances in the structural understanding of αAChR peptides in complex with α-BTX, the boundaries of the binding domain on the receptor are uncertain to date. While previous studies have been instrumental in locating this domain within the 32-mer segment, a systematic residue-by-residue truncation experiment has not been performed, and the precise boundaries of the binding domain remain undetermined. A comparison of the competitive inhibition of α-BTX binding to AChR by the aforementioned 12-mer (residues 185−196, $IC_{50} = 1.3 \times 10^{-5}$ M), 18-mer (residues 181−198, $IC_{50} = 9.3 \times 10^{-6}$ M), and 32-mer (residues 173−204, $IC_{50} = 1.4 \times 10^{-7}$ M) (*21*) indicates that significant contact area is contributed by residues outside the shorter segments. These findings underline the need for structural studies of α-BTX complexes with longer peptide analogues of αAChR, capable of addressing the relevant structural questions at atomic resolution.

A complete high-resolution structure of AChR has not been solved yet due to the difficulties in crystallizing this membrane protein. Different models of αAChR disagree on the presence of secondary structure in the α-BTX-binding domain (*32*−*34*). Tritium hydrogen exchange kinetics of the AChR have been analyzed, and retardation in the exchange rate was observed in the presence of α-BTX (*35*). It was suggested that α-BTX shields the AChR by forming an intermolecular β-sheet, thereby decreasing solvent accessibility. Circular dichroism (CD) measurements of a peptide corresponding to residues 185−196 of the αAChR indicated an increase of β-structure upon α-BTX binding (*36*).

In this study, we use the sensitivity of the homonuclear Hartmann−Hahn (HOHAHA) and rotating-frame Overhauser spectroscopy (ROESY) NMR experiments to the $T_{1\rho}$ relaxation time of the detected protons. Peptide protons interacting with the toxin are immobilized upon binding and assume a $T_{1\rho}$ relaxation time comparable to that of the toxin protons. Peptide protons with no interaction with the toxin retain some mobility and have considerably longer $T_{1\rho}$ relaxation time. The mixing period in the HOHAHA and ROESY experiments is tuned to discriminate between the immobilized and flexible peptide protons, thus enabling us to accurately locate the α-BTX-binding domain on the αAChR. Standard 2D-NMR techniques are applied to determine the secondary structure of the αAChR peptide in the binding site of α-BTX. Identification of the complete linear segment in αAChR recognized by α-BTX and determination of its secondary structure are a prerequisite for detailed structural studies by NMR or X-ray crystallography. In this study, we map the determinant of the αAChR involved in strong α-BTX binding, and elucidate the secondary structure of the αAChR peptide bound to α-BTX.

EXPERIMENTAL PROCEDURES

Peptide Synthesis and Complex Formation. The peptides αp22 (KEARGWKHWVFYSCCPTTPYLD) and αp25 (EERGWKHWVYYTCCPDTPYLDITEE), comprising residues 179−200 of mouse and residues 182−202 of *Torpedo* AChR, respectively, were synthesized on an AMS422 automated multiple peptide synthesizer (Gilson) and purified by RP-HPLC. αp25 was elongated by two glutamic residues at each terminus to increase peptide solubility. Formation of the ^{R}C192−^{R}C193 disulfide bond was ensured for both peptides, emulating their oxidation state in the native AChR (*37*), although this state has little effect on α-BTX binding (*38*). In αp25, this disulfide bond was formed by air-oxidation in a dilute peptide solution (10 mg/250 mL) to avoid oligomerization (*39*). The Ellman reagent was used to monitor the completion of the reaction (*40*). αp22 was not treated, but its mass spectrum suggested it had oxidized during purification. The oxidized peptides were lyophilized and purified by RP-HPLC with an acetonitrile gradient. The composition of the peptides was verified by amino acid analysis, and their molecular mass and oxidation state were confirmed by mass spectrometry. α-BTX was purchased from Sigma. The α-BTX/αp22 complex was prepared by mixing the peptide and α-BTX at a molar ratio of 0.75:1, respectively. The α-BTX/αp25 complex was prepared by addition of excess oxidized αp25 to α-BTX. To obtain a 1:1 complex of α-BTX and αp25, this complex was purified by gel-filtration FPLC on a Pharamcia S-75 gel filtration column, using 250 mM NH_4HCO_3 as running buffer, followed by lyophilization. The formation of the complexes was verified by polyacrylamide gel electrophoresis, transverse NMR relaxation time (T_2) measurements, and dynamic light scattering. Complex formation was also monitored by the disappearance of the ^{B}H4(H^{δ}) and the ^{B}W28(H^{N})

resonances of the free toxin at 6.32 (*29*) and 8.6 ppm, respectively.

Dynamic Light Scattering Measurements. Dynamic light scattering measurements were performed using a Dynapro Molecular Sizing instrument at 25 °C. The concentration of all protein solutions was ~2 mg/mL. The molecular weight of α-BTX and the complexes was determined at several pH values and at various salt concentrations.

NMR Sample Preparation. αp22 was dissolved in a solution of 90% H_2O, 10% D_2O, and 0.05% NaN_3 and acidified with HCl to pH 3.8. αp25 was dissolved in a solution of 80% H_2O, 10% D_2O, and 10% CD_3CO_2H. The final concentration of peptide samples was 2 mM. The α-BTX/peptide complexes were shown by DLS and T_2 measurements to exist in a monomeric state at pH 4, and therefore all complexes were dissolved in 90% H_2O/10% D_2O and 0.05% NaN_3 and acidified to this pH with HCl. Final concentrations of α-BTX/αp22 and α-BTX/αp25 samples were 1.8 and 2 mM, respectively. α-BTX/αp25 complex in 99.99% D_2O was prepared by two cycles of dissolving the lyophilized toxin in 99.8% D_2O, incubation at 42 °C for 14 h, lyophilization, and final dissolving in 99.99% D_2O. This sample was acidified to pH 4 using acetic acid-d_4.

NMR Measurements. All NMR spectra were acquired on Bruker DMX-500 MHz and DRX-800 MHz spectrometers. Amide proton T_2 measurements were conducted at various pH values and 30 °C using a 1,1-echo sequence. The pulse sequence used for the 2D HOHAHA measurements combined a WALTZ (*42*) or DIPSI-2 (*43*) sequence for isotropic mixing, sensitivity enhancement (*44*) using Echo/Anti-echo-TPPI gradient selection (*44*) and a 3-9-19 pulse sequence with gradients for water suppression (*45*). ROESY and NOESY measurements used States-TPPI for phase sensitivity and the WATERGATE (WATER suppression by GrAdient-Tailored Excitation) or 3-9-19 sequences for water suppression (*45*, *46*). The DQF-COSY spectrum was acquired by conventional procedures (*47*).

HOHAHA, ROESY, and NOESY spectra of αp22 were acquired at 20 °C using mixing times of 150, 150, and 300 ms, respectively. For αp25, HOHAHA spectra were acquired at 30 and 47 °C. Sequential assignment of αp22 and αp25 was performed according to the well-established method of Wüthrich (*48*).

To determine the binding domain, HOHAHA and ROESY spectra of the α-BTX/αp22 and α-BTX/αp25 complexes were acquired with varying mixing times of 100−400 ms, 2−4K points in the F_2 and 256−600 increments in the F_1 dimensions at 20 and 30 °C. Sequential assignment of the observed peptide spin systems of the α-BTX/αp22 complex was performed using the HOHAHA and ROESY spectra with a mixing time of 400 ms. Sequential assignment of the observed peptide spin systems of the α-BTX/αp25 complex was performed using the HOHAHA and ROESY spectra with a mixing time of 250 and 200 ms, respectively.

For the complete sequential assignment of the α-BTX/αp25 complex, HOHAHA and NOESY spectra with 8K data points in F_2 and 800 increments in F_1 were acquired with mixing times of 70 and 150 ms, respectively, at 30 and 37 °C. The AURELIA software package (*49*) was used to determine the relative intensities of the sequential NOEs. For assignment of the aliphatic region in 99.99% D_2O, HOHAHA and NOESY spectra with water presaturation were acquired at 37 °C with mixing times of 70 and 150 ms, respectively.

To identify slowly exchanging amide protons, the α-BTX/αp25 complex was lyophilized from H_2O and redissolved in 99.8% D_2O at pH 4.1 (uncorrected for isotope effects). A series of six HOHAHA experiments at 37 °C, each 2.5 h long, was initiated 45 min later. Amide protons still giving rise to cross-peaks after 3 h were considered to be in slow exchange with the solvent.

$^3J_{HNH\alpha}$ couplings of free αp22 and αp25 were measured from the HOHAHA spectrum acquired with a mixing time of 150 ms at 20 °C with 4K (zero-filled to 8K) points in F_2 and 400 increments in the F_1 dimension. $^3J_{HNH\alpha}$ couplings of the αp25/α-BTX complex were measured from a DQF-COSY spectrum acquired at 37 °C with 8K (zero-filled to 16K) points in F_2 and 1024 increments in the F_1 dimension. The AURELIA software package (*49*) was used to fit the anti-phase doublets and obtain the J couplings.

RESULTS

Optimization of Measurement Conditions. To determine the optimal pH of the α-BTX/peptide complexes for NMR experiments, a series of dynamic light scattering (DLS) measurements at increasing pH values were performed. At pH 4, the measurements displayed a molecular mass of 11.2 kDa, consistent with the monomeric state of the α-BTX/αp25 complex. However, at pH ≥5, the complex exhibited a mass of ~20 kDa, implying it had dimerized as suggested in several studies where α-BTX was a homodimer (*50*, *51*). Furthermore, salt concentrations up to 0.25 M did not significantly inhibit dimerization. These findings were further supported by T_2 relaxation time measurements of the complexes. T_2 values of 13−20 ms were measured at pH 6, indicating that indeed dimerization had occurred. At pH 4, however, the complexes displayed T_2 values of 35−40 ms, the expected value for a monomeric complex of 11.2 kDa. It has been previously shown that the complex maintains its structure at this pH (*29*), and pH 4 was therefore chosen for NMR measurements of all complexes.

Mapping the N-Terminus of the α-BTX-Binding Determinant. To map the N-terminus of the αAChR segment recognized by α-BTX, a set of HOHAHA spectra with mixing periods of 300, 350, 400, 500, and 600 ms were acquired for the α-BTX/αp22 complex. The HOHAHA and ROESY spectra measured with a mixing time of 400 ms retained the cross-peaks of the mobile part of the αAChR peptide with good signal-to-noise ratio, while the contribution of the toxin cross-peaks was minimal (Figure 1). Using these spectra, five residues (^{R}E180−^{R}W184) of αp22 could easily be assigned, as well as the cross-peaks arising from ^{R}K185-($H^{N\epsilon}$) (not shown). Proton chemical shifts of residues ^{R}E180−^{R}G183 were practically identical to those observed for the free peptide, indicating they are flexible and do not participate in α-BTX binding. The chemical shifts of ^{R}W184(H^{α}) and ^{R}K185($H^{N\epsilon}$) differ from those of the free peptide by 0.1 and 0.25 ppm, respectively, and their HOHAHA cross-peaks were very weak, indicating that these residues are within the AChR determinant recognized by α-BTX. The cross-peaks of ^{R}H186−^{R}Y198 were undetectable in the spectra. We therefore concluded that N-terminal residues ^{R}K179−^{R}G183 lie outside the determinant recognized by α-BTX,

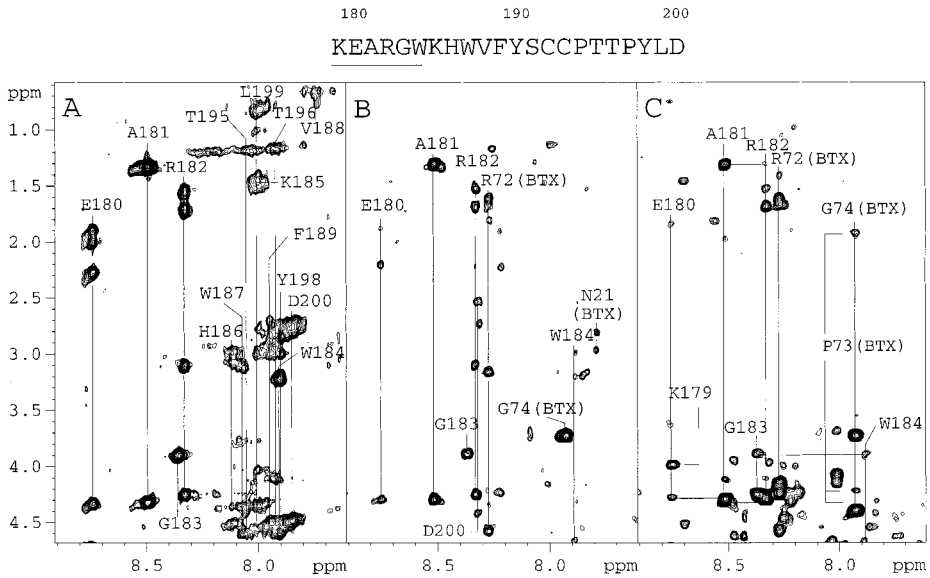

FIGURE 1: Dynamic filtering spectra. (A) HOHAHA spectrum of free αp22 acquired with a mixing time of 150 ms. (B) HOHAHA spectrum of the α-BTX/αp22 complex acquired with a mixing time of 400 ms. (C) ROESY spectrum of the α-BTX/αp22 complex acquired with a mixing time of 400 ms. Above the figure is the αp22 sequence, and underlined are the residues implicated as being flexible. All spectra were measured at 20 °C in 10% D_2O/90% H_2O and at pH 4.

and that ^{R}W184 is at the boundary of this determinant. The C-terminal residues ^{R}L199 (not shown in Figure 1) and ^{R}D200 gave rise to weak cross-peaks in the HOHAHA spectra with 400 ms mixing time, and their assignment was possible using the ROESY spectrum with shorter mixing time (200−300 ms), suggesting they are somewhat flexible. However, the change in their proton chemical shifts implied that they do interact with α-BTX. Determination of the C-terminal boundary of the binding determinant for α-BTX using this peptide was therefore inconclusive, because the ^{R}L199−^{R}D200 residues could be subject to terminal effects, and residues downstream of ^{R}D200 could participate in the binding. Cross-peaks arising from the mobile C-terminal residues of α-BTX were also detected in the long mixing time spectra. They were differentiated from peptide protons based upon the assignment of the library peptide/α-BTX complex and arise from residues ^{B}K70−^{B}G74 (*30*). This assignment was later verified by the complete assignment of the α-BTX/peptide complexes.

Mapping the C-Terminus of the α*-BTX-Binding Determinant*. The above results suggested that a longer peptide was necessary to determine the C-terminus of the α-BTX-binding determinant. A 29 residue peptide, RGWKHWVYYTCCPDTPYLDITYHFIMQRI, corresponding to residues 182−210 of the *Torpedo* αAChR, was insoluble in water, and no complex with α-BTX was obtainable. To increase peptide solubility, four C-terminal residues (MQRI) were omitted and two glutamic acid residues were added at each terminus. The resulting peptide, EERGWKHWVYYTCCPDTPYLDITYHFIEE, was soluble at basic pH, but precipitated at the acidic pH required for controlled complex formation. To increase the solubility at acidic pH, four additional C-terminal residues (YHFI) were omitted. The resulting peptide, αp25, was soluble at both acidic and basic pH, and a 1:1 complex with α-BTX could easily be obtained and purified as indicated by a decrease in the retention volume of the toxin observed on a Pharmacia S-75 gel filtration column before (14 mL) and after complexation (12.5 mL). DLS measurements of the molecular mass of α-BTX/αp25 concurred with the expected value of 11.2 kDa. Furthermore, longer T_2 relaxation times of 36 ms were measured for the complex, corresponding to molecular masses of 10−15 kDa. Several HOHAHA spectra were acquired with varying mixing times. The spectrum measured with a 250 ms mixing time showed a number of peptide cross-peaks with high signal-to-noise-ratio while only a limited number of α-BTX cross-peaks were observed. The peptide cross-peaks corresponded to residues which retained a longer $T_{1\rho}$ relaxation time upon complexation with α-BTX and were assigned to ^{R}E181−^{R}W184 and ^{R}I201−^{R}E204 using the ROESY spectrum measured with 200 ms mixing (Figure 2). We therefore concluded that the determinant recognized by α-BTX comprised residues W^{184}KHWVYYTCCPDTPYLD^{200} of the *Torpedo* αAChR.

Sequential Assignments of the α*-BTX/*α*p25 Complex Resonances*. The resonances of all residues in the α-BTX/αp25 complex were assigned using the common sequential assignment technique (*48*). The assignment was facilitated by the enhanced sensitivity and resolution of the 800 MHz spectrometer, together with the improved measurement conditions of the sample consisting of the monomeric state of the 11.2 kDa complex. Resonances in the amide region were assigned utilizing NOESY and HOHAHA spectra recorded in H_2O with mixing times of 150 and 70 ms, respectively. Assignment of the aliphatic region was performed in the corresponding spectra recorded in D_2O. Figure 3 shows the TOCSY spectrum of the α-BTX/αp25 complex used in this study. In this spectrum, the amide protons are spread over a large spectral width of 4 ppm, thus significantly reducing resonance overlap and simplifying the assignment procedure. The majority of the α-BTX resonances did not change their chemical shift upon peptide binding (*52*), and were comparable to the assignment obtained by Hawrot and co-workers (*31*). α-BTX residues exhibiting significant changes in chemical shift (>0.2 ppm) were ^{B}H4, ^{B}T6, ^{B}A7, ^{B}T8, ^{B}S9, ^{B}I11, ^{B}N21, ^{B}L22, ^{B}W28, ^{B}C29, ^{B}D30, ^{B}F32, ^{B}G37, ^{B}K38, ^{B}V40, ^{B}E41, ^{B}C48, ^{B}Y54, ^{B}K70, and ^{B}Q71, most of which are directly involved in αAChR peptide binding (*31*, our unpublished results). Furthermore, due to a partial

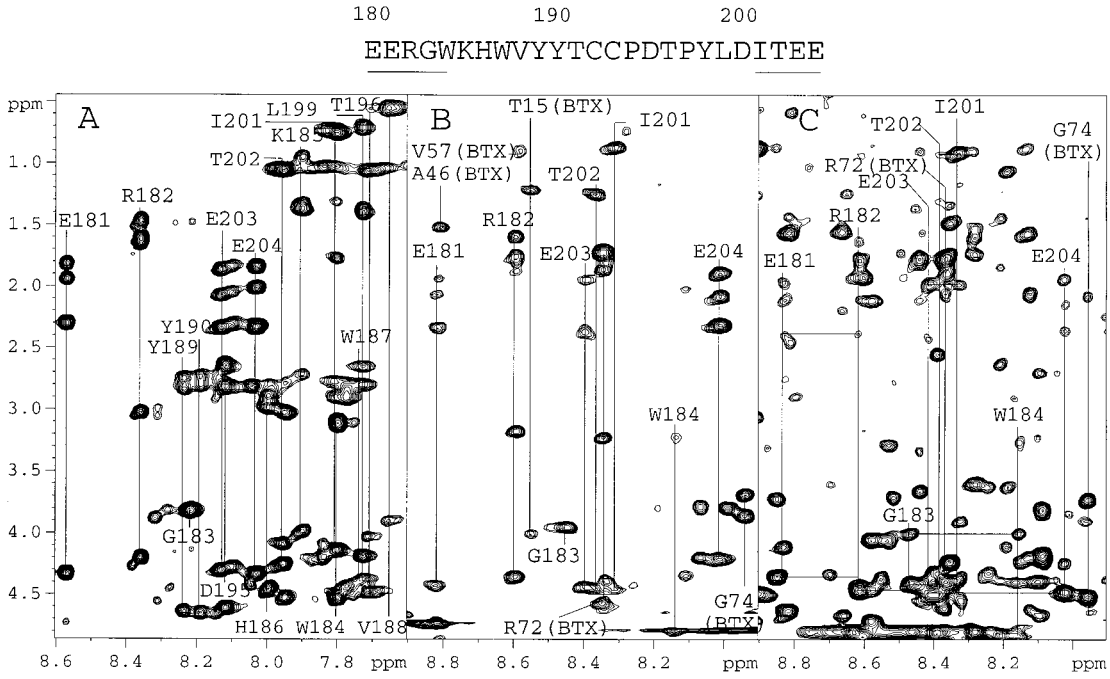

FIGURE 2: Dynamic filtering spectra. (A) HOHAHA spectrum of free αp25 acquired with a mixing time of 125 ms in 10% CD_3CO_2H. (B) HOHAHA spectrum of the α-BTX/αp25 complex acquired with a mixing time of 250 ms. (C) ROESY spectrum of the α-BTX/αp25 complex acquired with a mixing time of 200 ms. Above the figure is the αp25 sequence, and underlined are the residues implicated as being flexible. All spectra were measured at 20 °C. The spectra shown in panels B and C were measured in 10% D_2O/90% H_2O at pH 4.

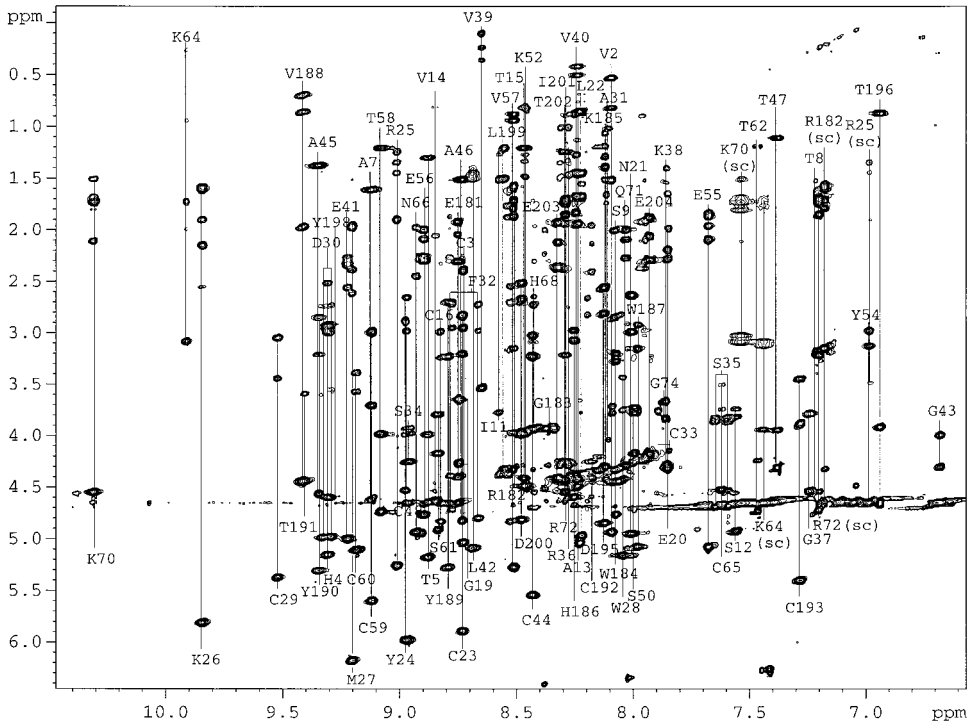

FIGURE 3: HOHAHA spectrum of the α-BTX/αp25 complex in H_2O. The spectrum of this 11.2 kDa complex was acquired at 37 °C and pH 4 with a mixing time of 70 ms. Lines denote the individual spin-systems.

mutation of A31V in the commercially available α-BTX (*53*), sequential assignment of five neighboring residues in the sequence (residues ^{R}D30−^{R}S35) was complicated, as they appeared twice. The amide protons of residues ^{B}T8 and ^{B}D63 appeared only in the NOESY spectra. Peptide residues lying outside the binding determinant exhibited chemical shifts identical to those of the free αp25, while residues within the binding region experienced changes in chemical shift. The sequential assignment pathway of the αp25 peptide bound to α-BTX is shown in Figure 4. Overlap of cross-peaks originating from residues ^{B}R36, ^{B}K51, ^{R}I201, and ^{R}T202 was alleviated using the corresponding spectra recorded at 30 °C and the considerably simplified HOHAHA and ROESY spectra recorded with long mixing times in which ^{R}I201 and ^{R}T202 still showed strong cross-peaks while those corresponding to ^{B}R36 and ^{B}K51 disappeared.

Secondary Structure of αp25 and α-BTX in Complex. The determination of the secondary structure of the complex was

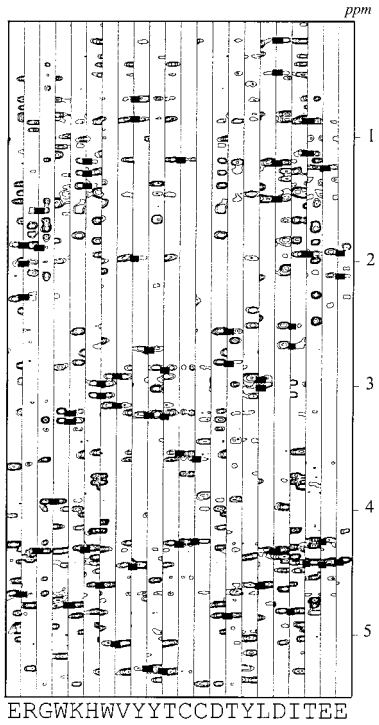

FIGURE 4: Sequential assignment pathway of the αAChR peptide, αp25, in the binding site of α-BTX. Shown are the strips of all non-proline αAChR residues in the ^{R}R182−^{R}T202 segment from the NOESY spectrum of the toxin/peptide complex. The spectrum was acquired in H_2O at 37 °C and at pH 4 with a mixing time of 150 ms. Filled boxes show the sequential connectivities. Assignment of ^{R}P194 and ^{R}P197 was based upon the aliphatic region of the spectrum (not shown).

based on the characteristics of different secondary structure elements and long-range NOEs. β-Sheets are typically characterized by strong $H^{\alpha}(i)/H^{N}(i+1)$ connectivities, by large (>8 Hz) $^{3}J_{HNH\alpha}$ couplings, by slowly exchanging amide protons, and by large (>0.3 ppm) positive deviation of the H^{α} chemical shifts from their random coil values (*48*). $^{3}J_{HNH\alpha}$ coupling constants were measured for α-BTX/αp25 residues, and the deviations of the H^{α} chemical shifts from their random coil values were calculated as well. These data, as well as sequential NOEs, solvent exchange data, and deduced secondary structure elements for the peptide/toxin complex, are summarized in Figure 5.

For the exact secondary structure determination of the α-BTX/αp25 complex, long-range $H^{N}(i)-H^{N}(j)$ and $H^{\alpha}(i)-H^{\alpha}(j)$ interactions ($|i - j| > 5$) were determined from the NOESY spectra in H_2O and D_2O, respectively (Figures 6 and 7). These interactions allow the determination of hydrogen-bond donors and acceptors, and together with additional $H^{N}-H^{\alpha}$ long-range NOEs summarized in Figure 8, confine the borders of the β-strands in the complex. The NMR results indicate that β-strands are formed by the peptide segments ^{R}H186−^{R}T191 and ^{R}Y198−^{R}D200 and the toxin segments ^{B}V2−^{B}T5, ^{B}S12−^{B}T15, ^{B}L22−^{B}D30, ^{B}G37−^{B}A45, and ^{B}E55−^{B}S60. The toxin global fold suggested by the data is in excellent agreement with known α-neurotoxin structures. Furthermore, the data suggest that the peptide, αp25, forms a β-hairpin with the two β-strands ^{R}H186−^{R}V188 and ^{R}Y198−^{R}D200, and the segment ^{R}Y189−^{R}T191 forms an intermolecular β-sheet with residues ^{B}K38−^{B}V40 of the second finger of α-BTX. The $(Cys)_2$-Pro-Xxx-Xxx-Pro motif typical of αAChR forms the loop at the tip of the β-hairpin. The high $^{3}J_{HNH\alpha}$ coupling constant measured for ^{R}D195 and ^{R}T196 (9.7 and 9.6 Hz, respectively) indicates that these two residues also assume an extended conformation. The slow solvent exchange rate of the amide protons of residues ^{R}Y190, ^{R}C192, and ^{R}C193 suggests that they are shielded by intrapeptide or peptide−toxin interactions. The secondary structure of unbound α-BTX was found to consist of three antiparallel β-strands, namely, segments ^{B}L22−^{B}W28, ^{B}V40−^{B}A45, and ^{B}E56−^{B}S60 (*52*, *54*). However, long-range NOE contacts summarized in Figure 8 together with solvent exchange data indicate that the three β-strands are elongated upon peptide binding to include residues ^{B}C29−^{B}D30, ^{B}G37−^{B}V39, and ^{B}E55.

DISCUSSION

In this study we applied NMR dynamic filtering (*55*, *56*) to map the αAChR determinant recognized by α-BTX, using two overlapping αAChR peptide analogues. In a previous study, a combination of HOHAHA and ROESY spectra with long mixing periods was used to map the gp120 epitope recognized by the HIV-1 neutralizing antibody 0.5β (*57*). The three-dimensional structure of the peptide complex with the Fv fragment of the antibody was later solved by NMR (*58*, *59*) and was in excellent agreement with the dynamic filtering results. This attests to the potential of this method in precisely mapping peptide segments interacting with a much larger protein.

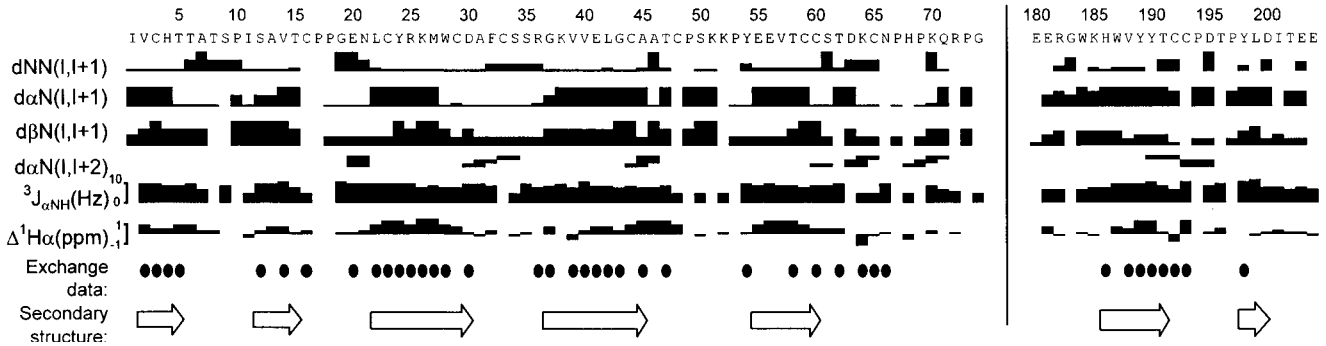

FIGURE 5: Summary of NMR data used for the sequential assignment procedure and the secondary structure determination of αp25 and α-BTX in complex. The data were obtained from a NOESY spectrum recorded at 37 °C and pH 4 with a mixing time of 150 ms. Indicated are the sequential NOE connectivities, with the line thickness indicating the relative volume integral of the cross-peak as determined by the AURELIA software package (*49*). $^{3}J_{\alpha NH}$ coupling constants and H^{α} chemical shift deviation from random coil values are shown. Filled circles represent slowly exchanging amide protons. Secondary structure elements deduced from these data are indicated as well.

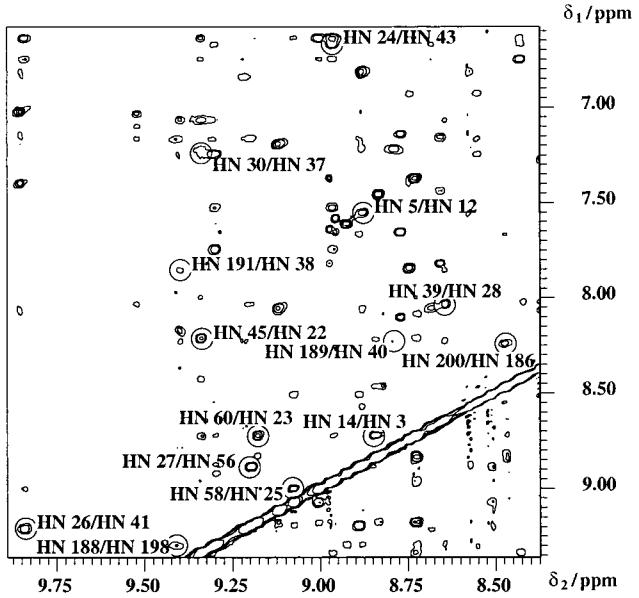

FIGURE 6: Region of the NOESY spectrum of the α-BTX/αp25 complex in H_2O at 37 °C and pH 4 with a 150 ms mixing time showing the long-range H^N-H^N interactions. Cross-peak numbers 1−74 and 180−204 follow toxin and peptide residue numbering, respectively. These NOEs were used to determine the secondary structure of the complex.

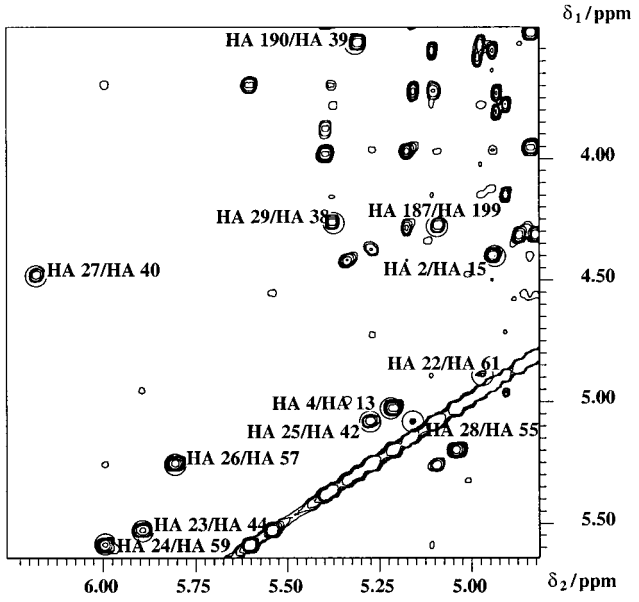

FIGURE 7: Region of the NOESY spectrum of the α-BTX/αp25 complex in D_2O at 37 °C and pH 4 with a 150 ms mixing time, showing the long-range $H^\alpha-H^\alpha$ interactions. Cross-peak numbers 1−74 and 180−204 follow toxin and peptide residue numbering, respectively. These NOEs were used to determine the secondary structure of the complex.

The current study pinpoints the major αAChR determinant interacting with α-BTX to residues ^{R}W184−^{R}D200. This segment was shown to bind α-BTX with a K_D of 2.5×10^{-7} M, similar to that of the denatured α-subunit to α-BTX. The shorter 184−196 αAChR segment exhibits a K_D of 4.7×10^{-6} M, indicating that the sequence 197−200 contributes to α-BTX binding (*25*). Mutations of ^{R}H186, ^{R}Y189, ^{R}Y190, ^{R}C192, ^{R}C193, ^{R}P194, and ^{R}D195 greatly reduced or abolished α-BTX binding, and mutation of ^{R}Y198 decreased the binding to a lesser extent (*27*). Affinity to α-BTX was conferred upon an α-BTX-insensitive α-subunit by introducing a cluster of five residues from the *Torpedo* sequence (^{R}W184, ^{R}W187, ^{R}V188, ^{R}Y189, and ^{R}T191), indicating that these residues are important for toxin binding (*60*). The binding sites for α-BTX and acetylcholine upon αAChR are known to overlap, and affinity-labeling studies implicated the invariant residues ^{R}C192, ^{R}C193 (*61*), ^{R}Y190, and ^{R}Y198 (*62*−*65*) as crucial for acetylcholine binding. Binding experiments using bacterially expressed overlapping peptides revealed that residues ^{R}P197−^{R}D200 contribute to α-BTX binding (*25*). Thus, a large number of residues within the 184−200 sequence including ^{R}W184 and ^{R}D200 have been implicated by various experimental methods as important for α-BTX binding.

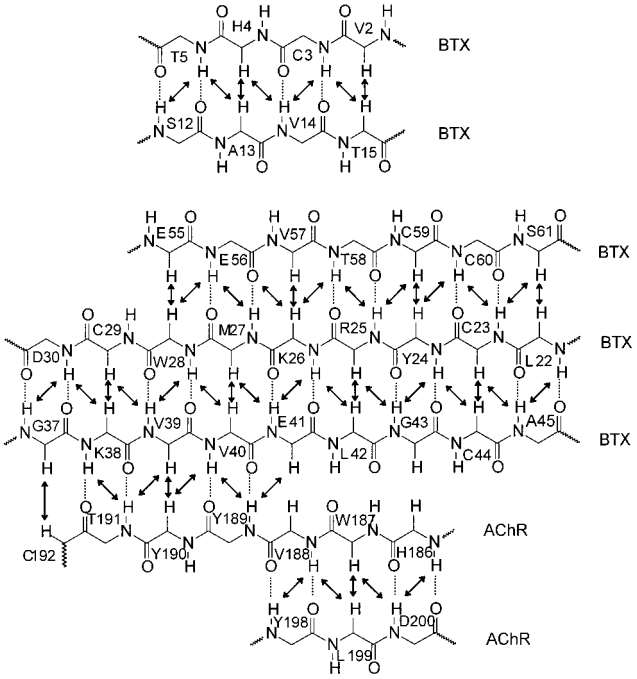

FIGURE 8: Secondary structure of αp25 in complex with α-BTX derived from NMR data. The toxin consists of a triple-stranded antiparallel β-sheet composed of segments ^{B}L22−^{B}D30, ^{B}G37−^{B}A45, and ^{B}E55−^{B}S61, and of an additional antiparallel β-sheet involving residues ^{B}V2−^{B}T5 and ^{B}S12−^{B}T15. αp25 folds into a β-hairpin conformation, in which residues ^{R}H186−^{R}V188 and ^{R}Y198−^{R}D200 form the two β-strands. Residues ^{R}Y189−^{R}T191 form an intermolecular β-sheet with segment ^{B}K38−^{B}V40 of α-BTX.

The observation that αp25 residues ^{R}R182, ^{R}G183, ^{R}I201, and ^{R}T202 and their flanking glutamates are highly flexible in comparison to the majority of α-BTX residues, and that α-BTX affinities to a peptide comprised of residues 184−200 and to denatured αAChR are similar (*25*), indicates that the αAChR residues adjacent to this sequence do not contribute to toxin binding. The high affinity of intact pentameric AChR to α-BTX ($K_D = 10^{-11}$ M) can be attributed to distal segments of the α-subunit as well as to residues in other subunits (*16*, *66*).

Several studies attempted to predict the secondary structure of αAChR. Finer-Moore and Stroud applied amphipathic analysis to αAChR and predicted a β-strand conformation for the ^{R}W184−^{R}D200 segment (*32*) with a turn formed by ^{R}C192 and ^{R}C193. Chaturvedi et al. (*27*) proposed a β-hairpin conformation in which ^{R}C192, ^{R}C193, and ^{R}P194 form a loop and all the other residues form β-strands. On the other hand, very recently Changeux and co-workers predicted no second-

ary structure for the ^{R}R182−^{R}D200 segment and a β-strand formed by residues ^{R}I201−^{R}M207 only (*34*). In another recent modeling study, Ortells et al. used 6 different prediction methods and 118 aligned sequences to extend this β-strand to include residues ^{R}Y198−^{R}I210, with residues ^{R}G183−^{R}P197 remaining unstructured (*33*). This controversy between the earlier and more recent secondary structure predictions emphasizes the importance and relevance of the experimental structural data presented in our study.

The NMR data provide evidence for a β-hairpin conformation in which residues ^{R}H186−^{R}V188 and ^{R}Y198−^{R}D200 form the two interacting β-strands, and residues ^{R}C192−^{R}P197 form the turn. The ^{R}Y189−^{R}T191 segment within the β-hairpin forms a β-sheet with the second finger of α-BTX. Basus and co-workers observed an extended conformation for the five N-terminal residues of the αAChR peptide ^{R}K185−^{R}T196 bound to α-BTX (*29*), but not the β-hairpin conformation, since ^{R}Y198−^{R}D200 was absent in their peptide. The intermolecular β-sheet formation has not been observed as well, although this type of interaction was postulated by Hawrot and co-workers (*31*).

The well-established importance of residues ^{R}Y198−^{R}D200 for α-BTX binding may be attributed either to direct interactions with the toxin or to stabilization of the binding domain conformation as a β-hairpin. Dynamic filtering is unable to independently distinguish between these two possibilities without the assistance of long-range NOE interactions. This distinction is less relevant, however, in light of the accumulated biological data, which strongly suggest that residues involved in stabilizing the β-hairpin conformation, particularly the ^{R}Y198−^{R}D200 segment, significantly increase α-BTX affinity (*70*). The α-BTX-binding determinant on the αAChR therefore includes segments in contact with the toxin and others that ensure the determinant assumes the conformation required for binding.

The β-hairpin structure of αp25 bound to α-BTX emulates that of the corresponding αAChR segment in complex with α-BTX. Designed by evolution to bind to the corresponding segment of αAChR, the α-BTX-binding site serves as a template and forces the flexible peptide to fold into a conformation similar to that of native αAChR. This enables the peptide to fit into the considerably more rigid binding site of α-BTX.

Our findings demonstrate that α-BTX undergoes a conformational change upon binding αp25. The β-sheet of the second finger of α-BTX is elongated to accommodate the peptide binding. Hawrot and co-workers have described that residues at the edge of the β-sheet of the second finger, ^{B}W28 and ^{B}V39, zip together upon binding of dodecapeptide 185−196 (*29*). However, in our structure with the longer peptide αp25, additional residues, ^{B}C29−^{B}D30 and ^{B}G37−^{B}K38, extend the β-sheet, illustrating the importance of ^{R}P197−^{R}D200 in stabilizing the complex. The concerted elongation of the second finger of the toxin and the formation of the intermolecular β-sheet upon peptide binding together account for the changes in chemical shift of residues ^{B}W28−^{B}D30 and ^{B}G37−^{B}E41 at the second fingertip.

NMR and X-ray structural data indicate that several members of the snake α-neurotoxin family share a similar structure. Notable are α-cobratoxin and erabutoxin, which exhibit the structural motif present in α-BTX. This common structure is characterized by three fingers with a protruding C-terminus around a central core composed of a triple-stranded antiparallel β-sheet (*67*−*69*). Most interesting is the homology in the second finger in the segment involved in β-sheet formation in the α-BTX complex with the αAChR peptide. Our findings suggest that α-neurotoxins bind the αAChR through an intermolecular β-sheet, accounting for their high affinity.

The off-rate of the ^{R}W184−^{R}D200 segment is very slow [$k_{off} = 1.128 \times 10^{-4}$ s^{-1} (*25*)]. The intermolecular β-strand/β-strand interaction which involves a number of hydrogen bond and side-chain/side-chain interactions probably contributes significantly to the binding energy and is responsible, at least in part, for the slow off-rate. This off-rate accounts for the unexpected detection of slowly exchanging amide protons of the αAChR peptide in complex with α-BTX. The low on-rate for this complex [$k_{on} \sim 8 \times 10^{3}$ s^{-1} (*25*)] indicates that complex formation is not diffusion-controlled, but must be accompanied by a conformational change. Free αp22 possesses $^{3}J_{HNH\alpha}$ coupling constants of 6−8 Hz (excluding ^{R}C192−^{R}C193) and small H$^{\alpha}$ chemical shift deviations from random coil values at pH 4, suggesting no highly populated secondary structure is present, and only upon binding does it adopt the β-hairpin conformation. At neutral pH, the free peptide aggregates and therefore the coupling constants could not be measured. Earlier CD measurements of αAChR peptides carried out at neutral pH indicated an increase in β-structure upon α-BTX binding, and significant percentage of β-strand conformation for the free peptide (*36*). This discrepancy may originate from the different measurement conditions used in both studies. The aggregation state of free αAChR peptide has not been investigated earlier. This aggregation, observed by NMR at neutral pH (data not shown), may involve intermolecular β-sheet formation, which accounts for the CD observation.

As stated earlier, our proposed secondary structure for the αAChR peptide in complex with α-BTX provides relevant information regarding the functionally important residues in αAChR and the mechanism of α-BTX binding, with various possible applications. Stabilization of the bound peptide conformation by backbone cyclization (*71*) or by hydrogen bond mimicry (*72*) may lead to an efficient antidote against the snake toxin α-bungarotoxin. A three-dimensional structure will clearly broaden our understanding of this interesting system. Proton T_2 relaxation times of the αp25/α-BTX complex indicate that it is suitable for structural determination by NMR, and such studies are underway. The αAChR segment comprising residues 184−200 is also the major determinant involved in acetylcholine binding. This segment of the receptor and possibly some of its adjacent residues (*73*) are also the target of αAChR agonists such as nicotine, suberyldicholine, carbamylcholine, and cytisine and of αAChR antagonists such as α-cobratoxin and *d*-tubocurarine. Understanding the structure of this determinant is the key to possible future biological and biomedical applications.

ACKNOWLEDGMENT

We thank Aviva Kapitkovski and Prof. Mati Fridkin for peptide synthesis, and Yehezkiel Haik for peptide purification.

SUPPORTING INFORMATION AVAILABLE

List of chemical shift assignments of the α-BTX/αp25 complex (2 pages). This material is available free of charge via the Internet at http://pubs.acs.org.

REFERENCES

1. Claudio, T., Paulson, H. L., Green, W. N., Ross, A. F., Hartman, D. S., and Hayden, D. (1989) *J. Cell Biol. 108*, 2277−2290.
2. Betz, H. (1990) *Neuron 5*, 383−392.
3. Unwin, N. (1993) *J. Mol. Biol. 229*, 1101−1124.
4. Blount, P., and Merlie, J. P. (1989) *Neuron 3*, 349−357.
5. Merlie, J. P., and Sebbane, R. (1981) *J. Biol. Chem. 256*, 3605−3608.
6. Blount, P., and Merlie, J. P. (1988) *J. Biol. Chem. 263*, 1072−1080.
7. Tzartos, S. J., Rand, D. E., Einarson, B. L., and Lindstrom, J. M. (1981) *J. Biol. Chem. 256*, 8635−8645.
8. Tzartos, S. J., Kokla, A., Walgrave, S. L., and Conti-Tronconi, B. M. (1988) *Proc. Natl. Acad. Sci. U.S.A. 85*, 2899−2903.
9. Barkas, T., Gabriel, J. M., Mauron, A., Hughes, G. J., Roth, B., Alliod, C., Tzartos, S. J., and Ballivet, M. (1988) *J. Biol. Chem. 263*, 5916−5920.
10. Stroud, R. M., McCarthy, M. P., and Shuster, M. (1990) *Biochemistry 29*, 11009−11023.
11. Lentz, T. L., and Wilson, P. T. (1988) *Int. Rev. Neurobiol. 29*, 117−160.
12. Holtzman, E., Wise, D., Wall, J., and Karlin, A. (1982) *Proc. Natl. Acad. Sci. U.S.A. 79*, 310−314.
13. Zingsheim, H. P., Barrantes, F. J., Frank, J., Hanicke, W., and Neugebauer, D. C. (1982) *Nature 299*, 81−84.
14. Fairclough, R. H., Finer-Moore, J., Love, R. A., Kristofferson, D., Desmeules, P. J., and Stroud, R. M. (1983) *Cold Spring Harb. Symp. Quant. Biol. 48*, 9−20.
15. Haggerty, J. G., and Froehner, S. C. (1981) *J. Biol. Chem. 256*, 8294−8297.
16. Arias, H. R. (2000) *Neurochem Int. 36*, 595−645.
17. Oswald, R. E., and Changeux, J. P. (1982) *FEBS Lett. 139*, 225−229.
18. Chatrenet, B., Tremeau, O., Bontems, F., Goeldner, M. P., Hirth, C. G., and Menez, A. (1990) *Proc. Natl. Acad. Sci. U.S.A. 87*, 3378−3382.
19. Kreienkamp, H. J., Utkin, Y. N., Weise, C., Machold, J., Tsetlin, V. I., and Hucho, F. (1992) *Biochemistry 31*, 8239−8244.
20. Wilson, P. T., Lentz, T. L., and Hawrot, E. (1985) *Proc. Natl. Acad. Sci. U.S.A. 82*, 8790−8794.
21. Wilson, P. T., Hawrot, E., and Lentz, T. L. (1988) *Mol. Pharmacol. 34*, 643−650.
22. Wilson, P. T., and Lentz, T. L. (1988) *Biochemistry 27*, 6667−6674.
23. Ralston, S., Sarin, V., Thanh, H. L., Rivier, J., Fox, J. L., and Lindstrom, J. (1987) *Biochemistry 26*, 3261−3266.
24. Conti-Tronconi, B. M., Tang, F., Diethelm, B. M., Spencer, S. R., Reinhardt-Maelicke, S., and Maelicke, A. (1990) *Biochemistry 29*, 6221−6230.
25. Aronheim, A., Eshel, Y., Mosckovitz, R., and Gershoni, J. M. (1988) *J. Biol. Chem. 263*, 9933−9937.
26. Neumann, D., Barchan, D., Safran, A., Gershoni, J. M., and Fuchs, S. (1986) *Proc. Natl. Acad. Sci. U.S.A. 83*, 3008−3011.
27. Chaturvedi, V., Donnelly-Roberts, D. L., and Lentz, T. L. (1993) *Biochemistry 32*, 9570−9576.
28. Ackermann, E. J., Ang, E. T., Kanter, J. R., Tsigelny, I., and Taylor, P. (1998) *J. Biol. Chem. 273*, 10958−10964.
29. Basus, V. J., Song, G., and Hawrot, E. (1993) *Biochemistry 32*, 12290−12298.
30. Scherf, T., Balass, M., Fuchs, S., Katchalski-Katzir, E., and Anglister, J. (1997) *Proc. Natl. Acad. Sci. U.S.A. 94*, 6059−6064.
31. Gentile, L. N., Basus, V. J., Shi, Q. L., and Hawrot, E. (1995) *Ann. N.Y. Acad. Sci. 757*, 222−237.
32. Finer-Moore, J., and Stroud, R. M. (1984) *Proc. Natl. Acad. Sci. U.S.A. 81*, 155−159.
33. Ortells, M. O. (1997) *Proteins: Struct., Funct., Genet. 29*, 391−398.
34. Le Novere, N., Corringer, P. J., and Changeux, J. P. (1999) *Biophys. J. 76*, 2329−2345.
35. McCarthy, M. P., and Stroud, R. M. (1989) *Biochemistry 28*, 40−48.
36. Qing-luo Shi, C. K. L., Lentz, T. L., Armitage, I. M., and Hawrot, E. (1988) *Biophys. J. 53*, 94a.
37. Kao, P. N., and Karlin, A. (1986) *J. Biol. Chem. 261*, 8085−8088.
38. McLane, K. E., Wu, X. D., Diethelm, B., and Conti-Tronconi, B. M. (1991) *Biochemistry 30*, 4925−4934.
39. Richalet-Secordel, P. M., Deslandres, A., Plaue, S., You, B., Barre-Sinoussi, F., and Van Regenmortel, M. H. (1994) *FEMS Immunol. Med. Microbiol. 9*, 77−87.
40. Ellman, G. L. (1959) *Arch. Biochem. Biophys. 82*, 70−77.
41. Sklenar, V., and Bax, A. (1987) *J. Magn. Reson. 74*, 469.
42. Shaka, A. J., Keeler, J., and Freeman, R. (1983) *J. Magn. Reson. 53*, 313−340.
43. Shaka, A. J., Lee, C. J., and Pines, A. (1988) *J. Magn. Reson. 77*, 274−293.
44. Cavanagh, J., and Rance, M. (1990) *J. Magn. Reson. 88*, 72−85.
45. Piotto, M., Saudek, V., and Sklenar, V. (1992) *J. Biomol. NMR 2*, 661−665.
46. Sklenar, V., Piotto, M., Leppik, R., and Saudek, V. (1993) *J. Magn. Reson., Ser. A 102*, 241−245.
47. Piantini, U., Sorensen, O., and Ernst, R. R. (1982) *J. Am. Chem. Soc. 104*, 6800−6801.
48. Wuthrich, K. (1986) *NMR of Proteins and Nucleic Acids*, Wiley, New York.
49. Neidig, K.-P., Geyer, M., Gorler, A., Antz, C., Saffrich, R., Beneicke, W., and Kalbitzer, H. (1995) *J. Biomol. NMR 6*, 255−270.
50. Oswald, R. E., Sutcliffe, M. J., Bamberger, M., Loring, R. H., Braswell, E., and Dobson, C. M. (1991) *Biochemistry 30*, 4901−4909.
51. Sutcliffe, M. J., Dobson, C. M., and Oswald, R. E. (1992) *Biochemistry 31*, 2962−2970.
52. Basus, V. J., Billeter, M., Love, R. A., Stroud, R. M., and Kuntz, I. D. (1988) *Biochemistry 27*, 2763−2771.
53. Kosen, P. A., Finer-Moore, J., McCarthy, M. P., and Basus, V. J. (1988) *Biochemistry 27*, 2775−2781.
54. Love, R. A., and Stroud, R. M. (1986) *Protein Eng. 1*, 37−46.
55. Cheetham, J. C., Redfield, C., Griest, R. E., Raleigh, D. P., Dobson, C. M., and Rees, A. R. (1991) *Methods Enzymol. 203*, 202−228.
56. Kustanovich, I., and Zvi, A. (1996) *Methods Mol. Biol. 66*, 25−37.
57. Zvi, A., Kustanovich, I., Feigelson, D., Levy, R., Eisenstein, M., Matsushita, S., Richalet-Secordel, P., Regenmortel, M. H., and Anglister, J. (1995) *Eur. J. Biochem. 229*, 178−187.
58. Tugarinov, V., Levy, R., Dahan-Schokoroy, A., and Anglister, J. (1999) *J. Biomol. NMR 13*, 193−194.
59. Tugarinov, V., Zvi, A., Levy, R., Hayek, Y., Matsushita, S., and Anglister, J. (2000) *Struct. Fold. Des. 8*, 385−395.
60. Levandoski, M. M., Lin, Y., Moise, L., McLaughlin, J. T., Cooper, E., and Hawrot, E. (1999) *J. Biol. Chem. 274*, 26113−26119.
61. Kao, P. N., Dwork, A. J., Kaldany, R. R., Silver, M. L., Wideman, J., Stein, S., and Karlin, A. (1984) *J. Biol. Chem. 259*, 11662−11665.
62. Dennis, M., Giraudat, J., Kotzyba-Hibert, F., Goeldner, M., Hirth, C., Chang, J. Y., Lazure, C., Chretien, M., and Changeux, J. P. (1988) *Biochemistry 27*, 2346−2357.
63. Galzi, J. L., Revah, F., Black, D., Goeldner, M., Hirth, C., and Changeux, J. P. (1990) *J. Biol. Chem. 265*, 10430−10437.
64. Cohen, J. B., Sharp, S. D., and Liu, W. S. (1991) *J. Biol. Chem. 266*, 23354−23364.
65. Middleton, R. E., and Cohen, J. B. (1991) *Biochemistry 30*, 6987−6997.

66. Osaka, H., Malany, S., Molles, B. E., Sine, S. M., and Taylor, P. (2000) *J. Biol. Chem. 275*, 5478−5484.
67. Low, B. W., Preston, H. S., Sato, A., Rosen, L. S., Searl, J. E., Rudko, A. D., and Richardson, J. S. (1976) *Proc. Natl. Acad. Sci. U.S.A. 73*, 2991−2994.
68. Corfield, P. W., Lee, T. J., and Low, B. W. (1989) *J. Biol. Chem. 264*, 9239−9242.
69. Walkinshaw, M. D., Saenger, W., and Maelicke, A. (1980) *Proc. Natl. Acad. Sci. U.S.A. 77*, 2400−2404.
70. Gershoni, J. M., Hawrot, E., and Lentz, T. L. (1983) *Proc. Natl. Acad. Sci. U.S.A. 80*, 4973−4977.
71. Gilon, C., Halle, D., Chorev, M., Selinger, Z., and Byk, G. (1991) *Biopolymers 31*, 745−750.
72. Roark, W. H., Roth, B. D., Holmes, A., Trivedi, B. K., Kieft, K. A., Essenburg, A. D., Krause, B. R., and Stanfield, R. L. (1993) *J. Med. Chem. 36*, 1662−1668.
73. Lentz, T. L. (1995) *Biochemistry 34*, 1316−1322.

BI0022689